Cite this paper: Vietnam J. Chem., **2021**, *59(2)*, 167-178 Article
DOI: 10.1002/vjch.202000091

Highly effective photocatalyst of TiO_2 nanoparticles dispersed on carbon nanotubes for methylene blue degradation in aqueous solution

Nguyen Duc Vu Quyen[1*], Dinh Quang Khieu[1], Tran Ngoc Tuyen[1], Dang Xuan Tin[1], Bui Thi Hoang Diem[1], Ho Thi Thuy Dung[2]

[1]Department of Chemistry, University of Sciences, Hue University, 77 Nguyen Hue Str., Hue City, Thua Thien Hue 49000, Viet Nam

[2]Hue Medical College, 01 Nguyen Truong To Str., Hue City, Thua Thien Hue 49000, Viet Nam

Submitted June 1, 2020; Accepted September 3, 2020

Abstract

In the present study, titania nanoparticles are highly dispersed on carbon nanotubes via hydrolysis process of tetra-isopropyl-orthotitanate $Ti[OCH(CH_3)_2]_4$ (TPOT). The obtained composite (TiO_2/CNTs) is characterized by modern methods. The anatase-TiO_2 phase is realized based on X-ray diffraction spectrum at different pHs of hydrolysis solution. The band gap of TiO_2/CNTs (E_g) is calculated by Tauc method using diffuse reflectance spectroscopy (DRS). The TiO_2/CNTs composite plays as an active photocatalyst for methylene blue (MB) decomposition in aqueous solution. The effect of time to photocatalytic ability of TiO_2/CNTs composite is described using Langmuir-Hinshelwood kinetic model. The values of enthalpy variation (ΔH), entropy change (ΔS) and Gibbs free energy variation (ΔG) of the decomposition of MB are determined from thermodynamic study. In the range temperature from 283 K to 323 K, the positive values of ΔH and negative value of ΔG confirms endothermic and spontaneous nature of MB degradation. With the increase of temperature, the reaction occurs more easily, which is proved by more negative values of Gibbs free energy calculated from Van't Hoff equation.

Keywords. TiO_2/CNTs composite, hydrolysis of titanium alkoxide, Langmuir-Hinshelwood kinetic, TiO_2/CNTs photocatalyst.

1. INTRODUCTION

Ecosystem is strongly impacted by water contamination due to wastewater without treatment from industrial factories and household wastewater from populous cities in the world. In many big cities in Vietnam, numerous rivers and ponds are heavily contaminated, that endangers to human life. The oustanding pollutants putting negative effects on human health are heavy metals, toxic organic compounds. Among them, soluble organic pigment contributes a large part in household water pollution. Therefore, it is essential to study simple methods to lighten contamination with the aim of creating a fresh environment. Recently, the adsorption, biological method and especially, photocatalytic decomposition are popularly employed to remove organic pigments from aqueous solution.

At present, the photocatalytic decomposition has attracted worldwide interest because of its high effectiveness in organic pigments removal. Titania (TiO_2) is considered as the best photocatalyst for the degradation of the pigments from wastewater due to its prominent features, such as low cost, high chemical stability, environmental friendly and efficient photoactivity.[1-4] Especially, the crystalline phases of anatase-TiO_2 exhibits the strongest photocatalytic activity.[5] However, the relatively large band gap energy of TiO_2 (about 3.2 eV) requires high energy for photoactivation, such as ultraviolet irradiation.[1,6] In addition, due to non-porous structure and charged surface, anatase-TiO_2 presents small adsorption capacity for organic pollutants which are non-polar.[6] The photocatalytic ability of TiO_2 is also lessened because of the electron/hole pair recombination. These disadvantages require the studies on modification of TiO_2 surface or diffusion of TiO_2 on a suitable surface.[7-9]

Carbon nanotubes (CNTs) with very high surface area create many active adsorption sites for the catalyst surface. CNTs also play as the trap to keep electrons transferred from valence band of semiconductor for a short time before come to

conduction band. So, the charge recombination will be hampered.[10,11] It is therefore of paramount to achieve TiO_2/CNTs composite from CNTs and TiO_2 in a controllable way.[12-17]

In almost of previous studies, CNTs were prepared by chemical vapour deposition (CVD) with the presence of hydrogen flow as reductant of catalyst in form of transition metal oxide.[18-22] In the present study, CNTs with high surface area are synthesized by CVD without hydrogen. The surface area of CNTs is enhanced by oxidation with potassium permanganate in order to form oxidized CNTs which is dispersed in tetra-isopropyl-orthotitanate (TPOT) solution. The outstanding synthesis method of TiO_2/CNTs composite is dispering of the resulting CNTs in TiO_2 sol. However, studies on the formation of anatase phase from the mixture of TiO_2 sol and CNTs are rarely reported, which is investigated here. In addition, band gap of the obtained material is determined by well-known Tauc method. The composite is applied for MB photocatalytic decomposition in aqueous solution. The thermodynamic and kinetic of the decomposition are clearly studied.

2. MATERIALS AND METHODS

2.1. Materials

The starting CNTs were prepared from LPG (Vietnam) via CVD without initial hydrogen flow as raw-material. The diameter of carbon tubes were in the range from 40 to 50 nm (figure 1A).[23]

The oxidized CNTs (ox-CNTs) were formed with the oxidant of $KMnO_4$ and H_2SO_4 mixture. Upon this functionalization step, the CNTs become shorter in long-axis direction, the tubes' surface is rough, and $–COO^–$ and $–OH^–$ groups are created on their surface (figure 1B). Those groups play an important role as active sites for TiO_2 bonding. The synthesis and oxidation procedures were shown in our previous study.[23]

The synthesis of TiO_2/CNTs composite is presented by the following process shown in Scheme 1. The solution of tetra-isopropyl-orthotitanate in isopropanol (solution A) and the mixture of ox-CNTs in distilled water (mixture B) were both stirred for 30 min and ultrasonicated for 2 hours with the aim of highly dispersing. After that, the drop-wise addition of the solution A to the mixture B was carried out with strongly stirring and mixture C was obtained. The ultrasonic treatment was applied for the mixture C until the TiO_2 nanocrystals were completely formed. Then, the mixture C was filtered, washed with distilled water and dried at 100 ^oC for 24 hours. TiO_2/CNTs composite was obtained after furnacing mixture C at 500 ^oC for 2 hours. The molar ratio of TPOT:CNTs was surveyed in the range from 2.5 to 20.0. The anatase-TiO_2 sample was prepared via the same procedure without CNTs.

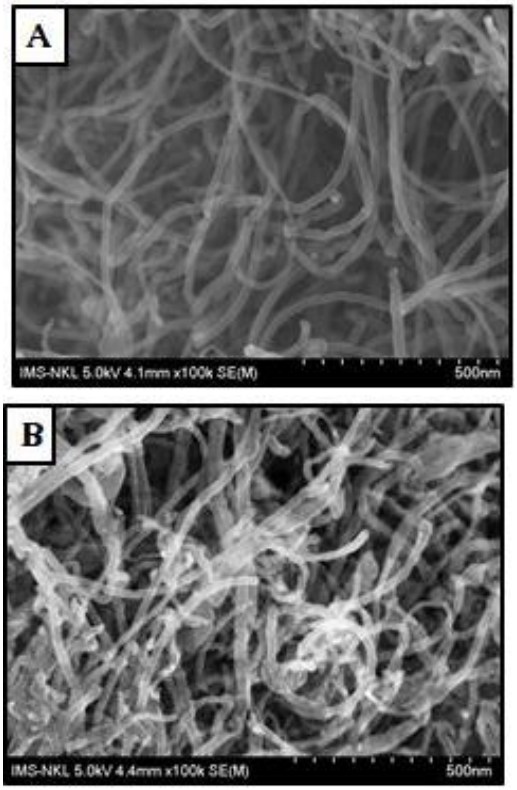

Figure 1: SEM images of pristine CNTs (A) and the oxidized CNTs (B)

2.2. Methods

2.2.1. Characterization of material

The crystal phase of the obtained TiO_2/CNTs composite was determined using X-ray diffraction (XRD) (RINT2000/PC, Rigaku, Japan). The elemental and functional group composition of CNTs were obtained from the energy-dispersive X-ray spectrum (EDS) (Hitachi S4800, Japan) and the Fourier transform infrared (FT-IR) spectroscope (Model IRPrestige-21 (Shimadzu, Kyoto, Japan)). The morphology of CNTs was observed using scanning electron microscopy (SEM) (Hitachi S4800, Japan). The band gap of TiO_2/CNTs composite (E_g) was determined using diffuse reflectance spectroscopy (DRS) (Cary 5000, Varian, Australia) with Tauc method.

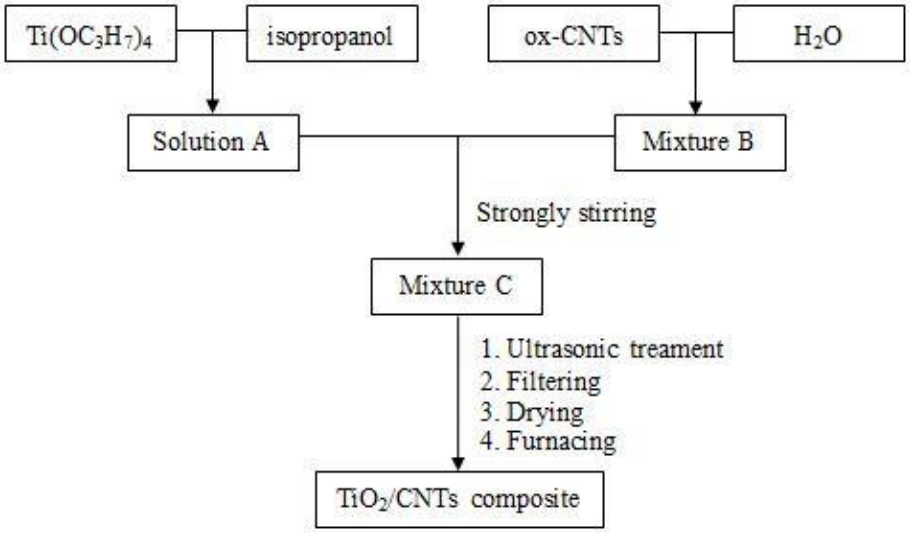

Scheme 1: The synthesis process of TiO_2/CNTs composite from $Ti(OC_3H_7)_4$ and CNTs

2.2.2. Catalytical studies

The degradation of MB by UV irradiation from a 20W lamp with a cut-off filter of 300-350 nm under the same condition can be detected as a measure standard of sample's photocatalytic activity. Before turning on the UV light, the suspension containing MB solution (50 mL, 20 mg L^{-1}) and TiO_2/CNTs photocatalyst (1.5 g L^{-1}) was magnetically stirred in dark with continuous stirring for 2 hours, this is to make sure that the physical adsorption gets equilibrium before the photocatalysis. MB concentration was determined using molecular absorption spectroscopy at wavelength of 660 nm. The standard curve method was employed to quantify MB concentration.

The effect of pH, catalyst dosage to MB degradation of TiO_2/CNTs composite and kinetic investigations were carried out. The pH of MB solution was adjusted from 3 to 11 by HNO_3 (0.1 mol L^{-1}) and NaOH (0.1 mol L^{-1}). The TiO_2/CNTs composite was added to the sample and the radiation was carried out. The content of MB before and after the photocatalytic degradation was determined. The dosage of TiO_2/CNTs catalyst was surveyed from 0.5 to 4.0 g L^{-1}. The kinetic data were inferred from the effect reaction times to the photocatalytic ability of TiO_2/CNTs with different MB initial concentrations from 10 to 50 mg L^{-1}.

The effect of temperature on MB degradation was studied from 283 to 323 K and thermodynamic parameters were determined. At each temperature, sample at pH of 8 containing MB solution (50 mL, 20 mg L^{-1}) was stirred with catalyst dosage of 1.5 g L^{-1} for different times. Consequently, activation parameters including the Gibbs free energy ($\Delta G^{\#}$), enthalpy ($\Delta H^{\#}$), entropy ($\Delta S^{\#}$) and activation energy (E_a) were determined from Arrhenius and Eyring equations. The thermodynamic parameters of photocatalytic reaction were obtained from Van't Hoff plot.

3. RESULTS AND DISCUSSION

3.1. Characterization of the composite

3.1.1. Crystal phase composition of material

The XRD patterns shown in figure 2 illustrate the crystalline phase of the obtained composite in the range of 2θ from 10° to 70°. The well-defined sharp diffraction peaks indicate highly crystalline nature of the material. The peaks at 2θ of 25.31°, 37.97°, 48.2°, 55.16° and 62.9° indexed as (1 0 1), (1 1 2), (2 0 0), (2 1 1) and (2 0 4) correspond to anatase phase TiO_2 with tetragonal structure, respectively.[24,25] The

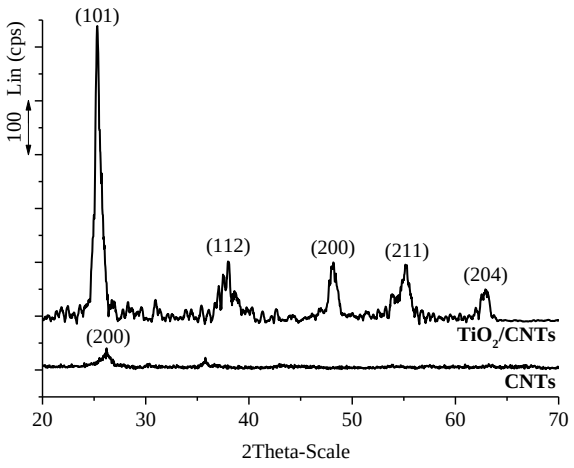

Figure 2: XRD pattern of pristine CNTs and TiO_2/CNTs composite obtained at hydrolysis pH of 8

peak at 2θ of 26.21° corresponding to crystal phase of CNTs might be overlapped with the peak at 2θ of 25.31°.

The best TiO_2/CNTs composite with suitable TPOP:CNTs molar ratio of 12.5 was obtained via hydrolysis method at hydrolysis pH of 8. At this pH, the highest MB degradation is achieved (92.67 %) because the most perfect anatase TiO_2 nanoparticles are formed. This is demonstrated through the investigation of the effect of hydrolysis pH to the formation of anatase phase shown in figures 3 and 4. The higher peak intensity is, the more perfect TiO_2 crystals are and the higher amount of anatase-TiO_2 phase is.[26] Figure 3 shows that at hydrolysis pH of 8, a larger amount of perfect TiO_2 crystals was formed, comparing to others. This result well fit with the highest MB degradation of TiO_2/CNTs composite obtained at hydrolysis pH of 8 (figure 4). That means TiO_2/CNTs composite with anatase form of TiO_2 synthesized via the hydrolysis of TPOT and well dispersed on CNTs, exhibits high photocatalytic activity.

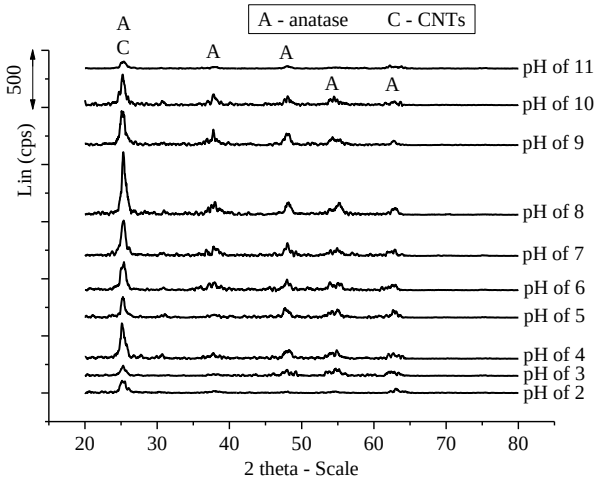

Figure 3: XRD patterns of TiO_2/CNTs composites obtained at different hydrolysis pHs

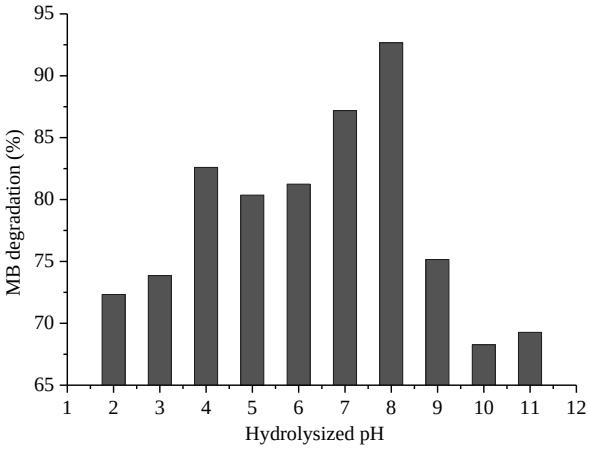

Figure 4: The MB degradation of TiO_2/CNTs composites obtained at different hydrolysis pHs

3.1.2. Morphology of material

The morphology of TiO_2/CNTs is realized on SEM observation shown in figure 5. Almost the nanotubes are highly dispersed with sphere TiO_2 nanoparticles (figure 5A) having a diameter around 20 nm (red circles in figures 5B, 5C, 5D). Some of TiO_2 aggregates are observed.

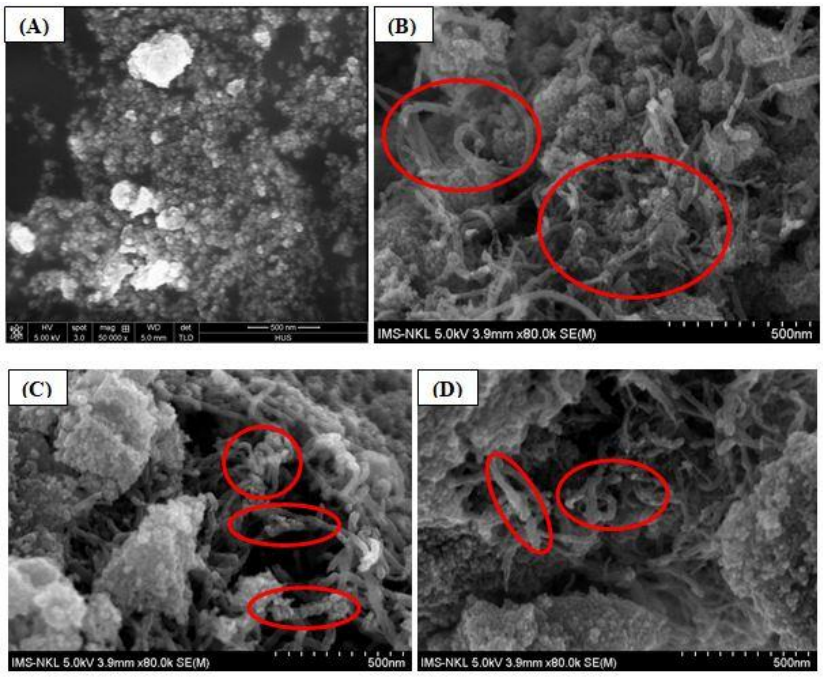

Figure 5: SEM images of TiO_2 nanoparticles (A) and TiO_2/CNTs composite (B, C, D)

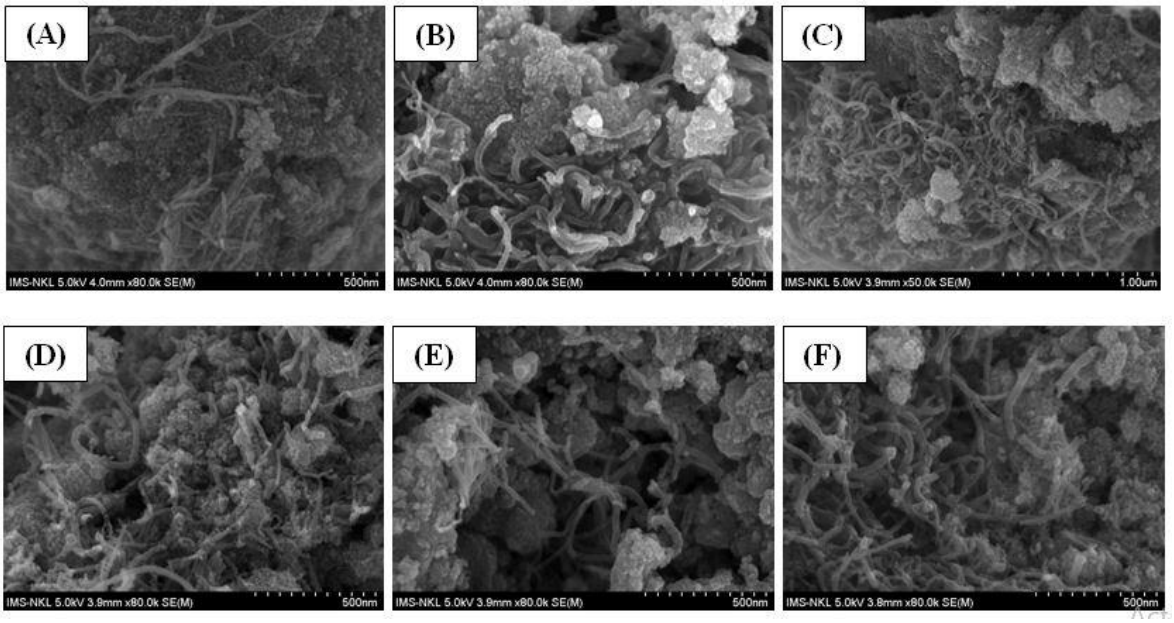

Figure 6: SEM images of TiO_2/CNTs composites synthesized with 0.5 (A); 1 (B); 1.5 (C); 2 (D); 2.5 (E); 3 (F) hours of ultrasonic treatment

Due to the close relationship between the dispersion of TiO_2 on nanotubes and MB degradation of the obtained catalyst, the study of ultrasonic treatment of the mixture after hydrolyzing TPOT was heeded. The effect of ultrasonic time to the dispersion of TiO_2 on nanotubes was surveyed from 0.5 to 3.0 hours under other same conditions. As can be seen, figure 6 reveals that TiO_2 nanoparticles are highly dispersed on CNTs following the increase of ultrasonic time from 0.5 to 2 hours and TiO_2 clusters become smaller. As a result, the MB degradation of TiO_2/CNTs raises from 50.7 to 92.2 % (figure 7). With the increase of ultrasonic time from 2 to 3 hours, the dispersion of TiO_2 on CNTs is well and photocatalytic activity seems to unremarkably vary.

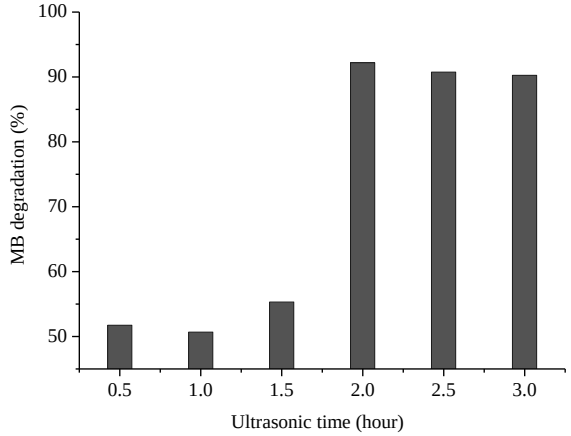

Figure 7: The MB degradation of TiO_2/CNTs composites synthesized with different ultrasonic times

3.1.3. Elemental and functional group compositions of material

EDS spectrum of TiO_2/CNTs composite is shown in figure 8A. As can be seen, the material comprises carbon, titanium and oxygen as main elemental composition. That demonstrates the presence of TiO_2 and CNTs in the material. The calculated amount of TiO_2 from EDS data (78.90 %) is not more different with the theoretical one (83.33 %). This partly confirms that TiO_2 nanoparticles are well dispersed on CNTs. The appearance of small amounts of Al and Fe on EDS spectrum infers the Fe_2O_3/Al_2O_3 catalyst of the fabrication of CNTs via chemical vapour deposition.

The appearance of $–COO^–$ and $–OH^–$ groups on CNTs and TiO_2/CNTs is studied using FT-IR spectroscopy (figure 8B). As can be seen, the absorption band attributed to $–OH^–$ groups appear at around 3464 cm^{-1}. Similarly, the band showing the presence of C-O groups is at around 1100 cm^{-1}. These groups might be from the surface oxidization of CNTs.[23] The weak peak at around 1600 cm^{-1} might attribute to C=C groups in the graphite structure. Especially, TiO_2 nanoparticles are realized based on the band assigned to Ti-O-Ti groups at around 690 cm^{-1}.

3.1.4. Band gap of material

Tauc method shows the relationship between E_g and absorption coefficient, according to equation (1):

$$\alpha h\nu = C_1(h\nu - E_g)^n \quad (1)$$

where C_1 is a proportionality constant; $h\nu$ is the energy of the incident photon, where h is Planck constant ($6.625x10^{-34}$ J s) and ν is wave number of photon; and n is a coefficient that depends on the kind of electronic transition, being, n = 1/2 for direct allowed transition, n = 3/2 for direct forbidden transition, n = 2 for indirect allowed transition, and n = 3 for indirect forbidden transition.[27]

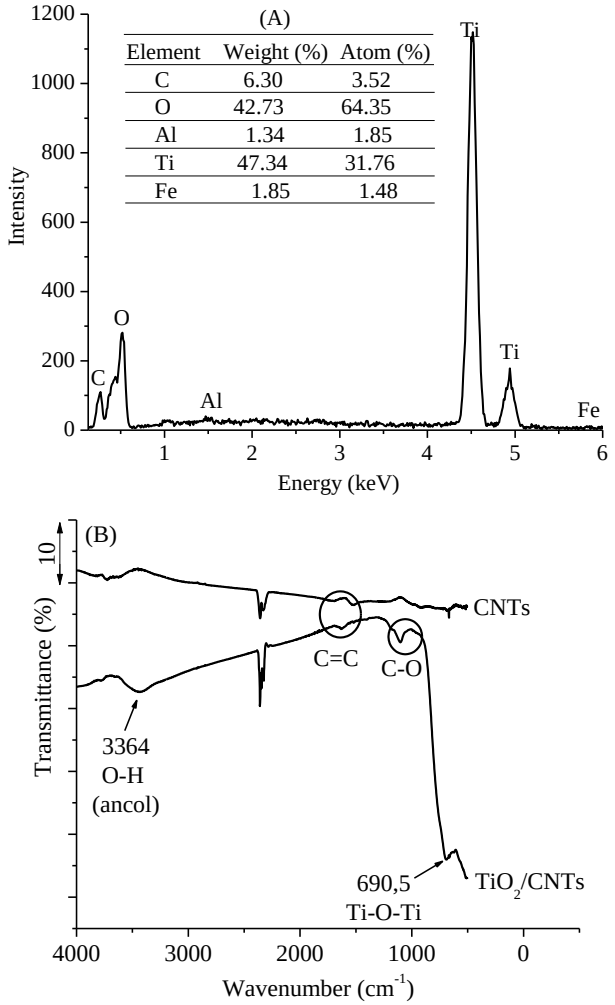

Figure 8: EDX (A) and FT-IR (B) spectra of TiO_2/CNTs composite

Using DRS, the analogous Tauc plots can be obtained, according to equations (2), (3), (4):

$$R_\infty = \frac{R_{sample}}{R_{standard}} \quad (2)$$

$$F(R_\infty) = \frac{K}{S} = \frac{(1-R_\infty)^2}{2R_\infty} \quad (3)$$

$$F(R_\infty)h\nu = C_2(h\nu - E_g)^n \quad (4)$$

where R_∞, is the reflectance of the sample with "infinite thickness", hence, there is no contribution of the supporting material, K and S are the absorption and scattering K-M coefficients, respectively, and C_2 is a proportionality constant.

From the reflectance (R_∞) of the sample, Tauc plot, $(F(R_\infty)h\nu)^2$ vs $h\nu$ (calculated from equations (2), (3) and (4)), is obtained and the band gap of TiO_2, CNTs and TiO_2/CNTs are determined as shown in Figure 9. The result shows that the presence of CNTs gives changes in the diffuse reflectance spectra. The band gap decreases from 3.16 eV for TiO_2-anatase to 2.84 eV for TiO_2/CNTs composite. The appearance of CNTs in TiO_2/CNTs composite therefore has two main effects: (i) the prevention of the electron/hole pair recombination; and (ii) the reduction of direct band gap of TiO_2.[4,28] Conclusion, an enhancement of the MB degradation in the experiments with TiO_2/CNTs composite (92.2 %) is observed when comparing with the experiments with TiO_2 alone (80 %) in the same conditions.

3.2. Photocatalytic activity of TiO_2/CNTs composite on decomposition of MB

3.2.1. Effect of pH and catalyst dosage

In aqueous solution, MB is in form of cation ($C_{16}H_{18}N_3S^+$)[29], pH of solution therefore influences the gathering of MB cations to catalyst surface. The higher amount of MB cations concentrated on catalyst surface provides the more advantage photocatalytic degradation of MB. The point of zero charge (PZC) of TiO_2/CNTs composite is 3.[30] If pH of solution is lower than PZC value, more H^+ ions will be formed than ^-OH ions in solution, and the surfaces of CNTs are positively charged and disadvantage to the attraction of cations. That means the pH below the PZC will be favourable for the adsorption of cations. The experimental data indicates that the enhancement of pH from 3 to 8 increases the negative charge on the surface of TiO_2/CNTs and strongly increases MB degradation of catalyst from about 17 % to more than 95 %. Then, MB degradation unremarkably rises with the increase of pH from 8 to 11.

The changing in MB photocatalytic degradation is investigated as a function of TiO_2/CNTs dosage amount from 0.5 to 4.0 g L^{-1}. With MB concentration of 20 mg L^{-1}, a strong uptrend of MB degradation is observed from 60.45 to 96.38 % when the amount of catalyst dosage increases from 0.5 to 1.5 g L^{-1}. Subsequently, the MB degradation slightly varies around the value of 96 %.

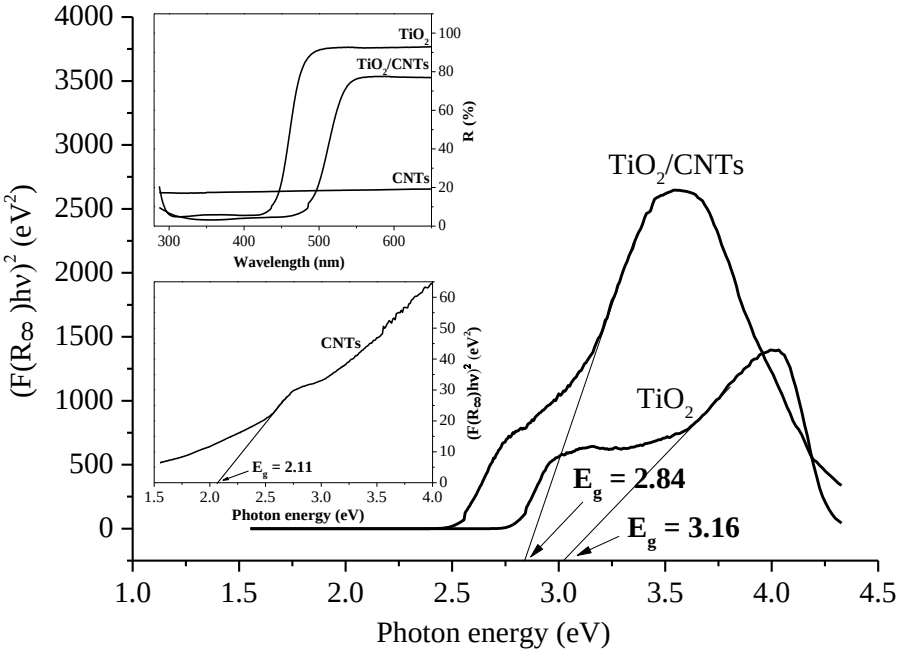

Figure 9: Tauc plots of TiO_2, CNTs and TiO_2/CNTs composite obtained from DRS analyses

3.2.2. Catalytic kinetic and thermodynamic studies

Figure 10 presents the reaction kinetics of the MB photocatalytic degradation with different initial concentrations of MB. The result shows that the longer contact time is, the higher MB degradation is. With the initial MB concentration increases from 10 to 50 mg L^{-1}, the efficiency of the decomposition decreases from around 96 % to around 82 % and the equilibrium reaction time increases from 75 to 120 min.

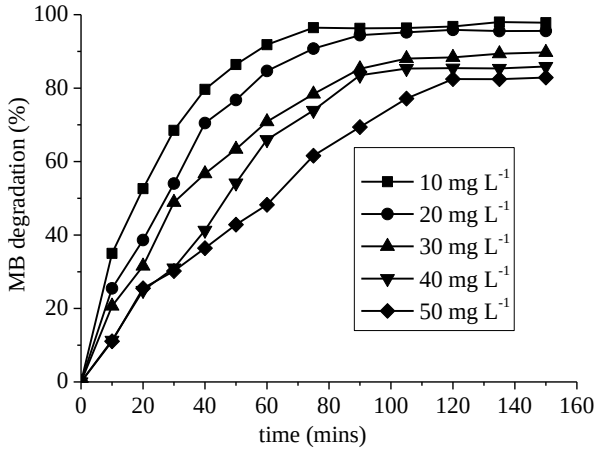

Figure 10: Effect of reaction time to MB degradation of TiO_2/CNTs composite at different initial MB concentrations

In order to describe the mechanism of heterogeneous catalytic reactions, the Langmuir-Hinshelwood (LH) kinetic model is employed.[31] According to this model, the reaction can be describes as follows:

$$\text{MB + catalyst} \Leftrightarrow \text{MB…catalyst} \quad (5)$$

$$\text{MB…catalyst} \rightarrow \text{products + catalyst} \quad (6)$$

where MB…catalyst is the activation complex formed prior to the product.

Among 2 above steps of the reaction, the equation (6) is assumed as the rate-limiting step. The LH expression was presented in our previous study.[31]

The adsorption of MB on the catalyst surface is assumed to be weak, LH equation becomes the first-order kinetic equation (equation (7)):

$$\ln\frac{C^0}{C} = k_1 t \quad (7)$$

where k_1 (min^{-1}) is the first-order rate constant.

All of the linear plots of the first-order kinetic equation obtained from experimental data at different initial MB concentrations from 10 to 50 mg L^{-1} (figure 11) represent high coefficients (0.980-0.998). This refers that the kinetic data fit well the first-order kinetics. That means, after adsorbing onto TiO_2/CNTs surface, MB molecules are immediately photocatalytic decomposed.

The value of k_1 is obtained from the slope of the linear regression line shown in table 1. The initial rate of reaction (r^0) is enhanced based on high initial MB concentration (C^0).[31] However, the rate constant of reaction (k_1) is reduced due to the unchanged mass of catalyst resulting the decrease in the number of catalytic sites.

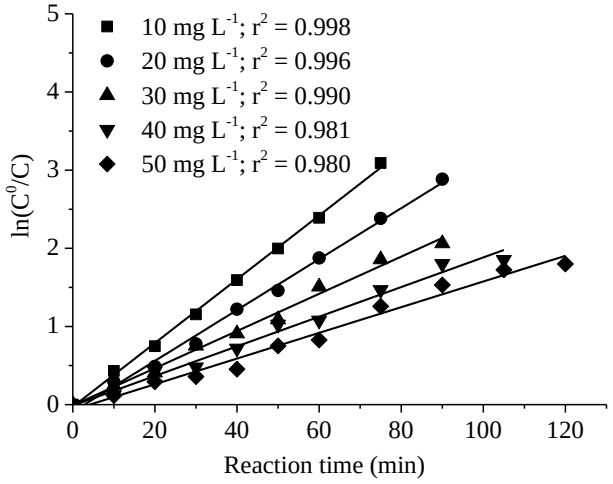

Figure 11: First-order kinetic study of the photocatalytic degradation of MB at different initial MB concentrations

Table 1: First-order kinetic parameters of the photocatalytic degradation of MB at different initial MB concentrations

C^0 (mg L^{-1})	k_1 (min^{-1})	r^0 (mg L^{-1} min^{-1})
10	0.0408	0.3655
20	0.0334	0.6576
30	0.0238	0.7152
40	0.0190	0.7425
50	0.0164	0.8108

From the experiment data in table 1, the linear plot of LH kinetic model is obtained (figure 12). The result proves high compatibility between the photocatalytic degradation data and LH kinetic model because the correlation coefficient of LH kinetic equation is nearly unity ($r^2 = 0.983$).

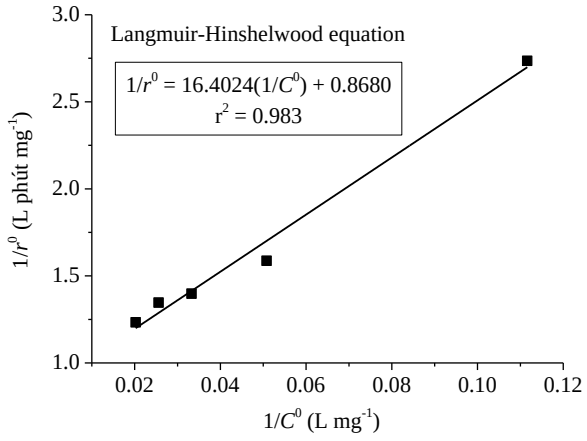

Figure 12: Langmuir-Hinshelwood kinetic model of the photocatalytic degradation of MB

In order to demonstrate the formation of intermediate prior to the adsorption, the thermodynamic parameters of activation including $\Delta H^{\#}$, $\Delta S^{\#}$, $\Delta G^{\#}$ are calculated based on linear form of Eyring equation.[31] The activation energy (E_a) is also determined by linear form of Arrhenius equation.[31]

The first-order kinetic equation is used to calculated the rate constants at different temperatures (k_T), as shown in figure 13 and table 2.

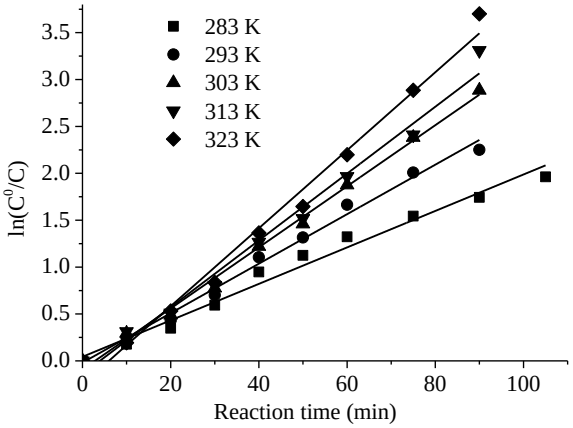

Figure 13: First-order kinetic studies of the photocatalytic degradation of MB at different temperatures

Table 2: First-order kinetic parameters of the photocatalytic degradation of MB at different temperatures

Temperature (K)	Correlation coefficient (r^2)	k_T (min^{-1})
283	0.9771	0.0192
293	0.9894	0.0266
303	0.9957	0.0334
313	0.9852	0.0369
323	0.9901	0.0463

Arrhenius and Eyring linear plots are obtained from k_T at different temperatures shown in Figure 14. Activation energy value calculated by the Arrhenius equation (figure 14A) is 15.94 kJ mol^{-1}. This value is below 42 kJ mol^{-1} which points out that the adsorption of MB molecules is quickly occurred onto catalyst surface, the intermediate is easily created, as a result of a strong decomposition of MB.

The values of activation parameters shown in table 3 are calculated from linear plot of Eyring equation (figure 14B). The formation of an intermediate or activated complex between MB and the catalyst is confirmed again due to the positive value of $\Delta S^{\#}$ (421.40 J mol^{-1} K^{-1}). The positive value of $\Delta H^{\#}$ (13.43 kJ mol^{-1}) suggests the endothermic nature of the formation of the activated complex. This intermediate is formed spontaneously and

favourable at high temperature because of the large negative values of $\Delta G^{\#}$. Therefore, MB photocatalytic decomposition is spontaneous and more favorable at high temperature. This is also demonstrated in table 2 that the reaction rate constant (k_T) of MB degradation increases with temperature and table 4 that the Gibbs free energy variations (ΔG^o) of MB degradation at different temperatures calculated from equation (8) have negative values.

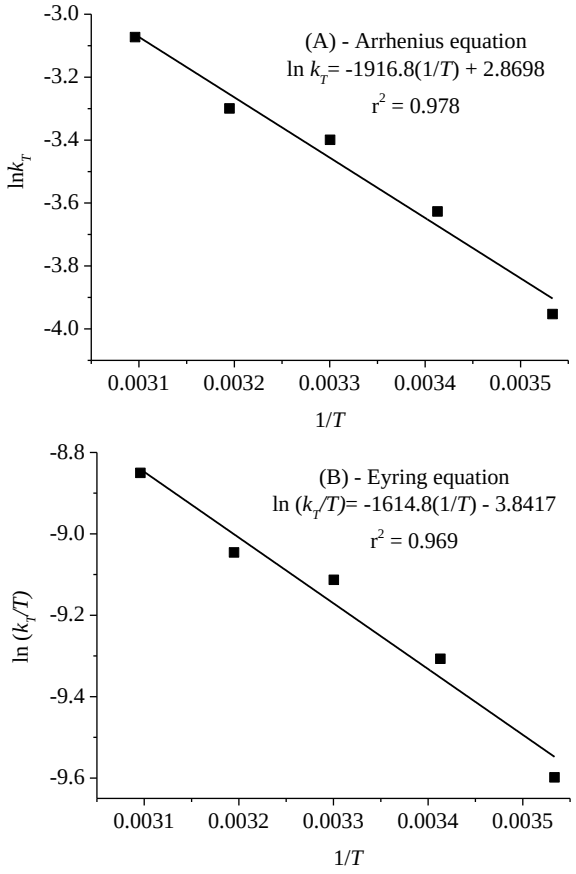

Figure 14: Arrhenius (A) and Eyring (B) equations for MB photocatalytic degradation

Table 3: Activation parameters for MB photocatalytic degradation

Temperature (K)	$\Delta H^{\#}$ (kJ mol^{-1})	$\Delta S^{\#}$ (J mol^{-1})	$\Delta G^{\#}$ (kJ mol^{-1})
283			-10.58
293			-11.00
303	13.43	421.40	-11.43
313			-11.85
323			-12.27

The enthalpy (ΔH^o) and entropy (ΔS^o) parameters were calculated using the Van't Hoff equation (equation (9) and figure 15).

$$\Delta G^o = -RT \ln K_C \quad (8)$$

$$\ln k_C = -\frac{\Delta G^o}{RT} = \frac{\Delta S^o}{R} - \frac{\Delta H^o}{RT} \quad (9)$$

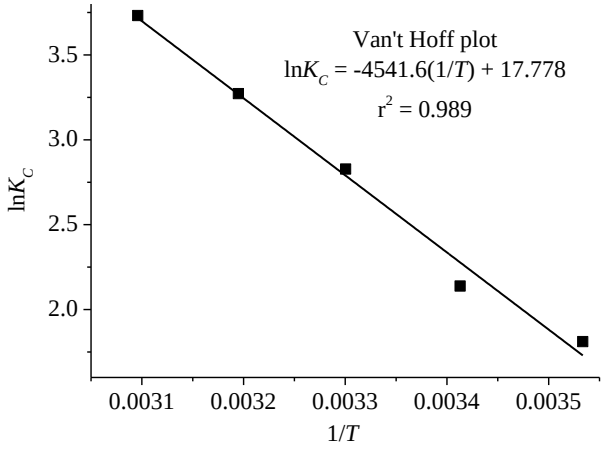

Figure 15: Van't Hoff plot for MB photocatalytic degradation

The endothermic nature of MB decomposition and the enhancement of the randomness at the liquid-solid interface are proved by the positive values of ΔH^o (37.76 kJ mol^{-1}) and ΔS^o (147.81 J mol^{-1} K^{-1}).

Table 4: Thermodynamic parameters of MB photocatalytic degradation

Temperature (K)	ΔH^o (kJ mol^{-1})	ΔS^o (J mol^{-1})	ΔG^o (kJ mol^{-1})
283			-4.07
293			-5.55
303	37.76	147.81	-7.03
313			-8.50
323			-9.98

According to plausible mechanism recommended by many studies, anatase-TiO_2 exhibits photocatalytic effectivity based on the generation of electron-hole pairs.[32-36] The increase of MB degradation of TiO_2/CNTs composite comparing to anatase-TiO_2 is explained that CNTs play as electron traps and attract MB molecules to catalyst surface. The proposed mechanism of MB degradation over TiO_2/CNTs composite can be described as in scheme 2. CNTs may accept the electrons (e^-) induced by UV irradiation from valence band in the TiO_2 nanoparticles and then, transfer them to the conduction band of TiO_2 nanoparticles. This process forms a positive charged hole (h^+) in valence band of TiO_2 nanoparticles. These electrons in conduction band may react with O_2 in the solution to form superoxide radical ion

($^{\bullet}O_2^-$) and these positive charged hole (h^+) may react with the OH^- derived from H_2O to produce hydroxyl radical ($OH^{\bullet}$). Consequently, these groups ($^{\bullet}O_2^-, OH^{\bullet}$) react with MB molecules to form non-toxic products, such as CO_2, H_2O, Cl^-, SO_4^{2-}, NH_4^+ and NO_3^-.[37] Therefore, it can be concluded that the appearance of CNTs extends living time of these electrons and holes, increases the gathering of positive charged MB ions on the surface of catalyst due to an active surface containing negative charged functional groups (COO^-, O^-) created from oxidization of CNTs by $KMnO_4/H_2SO_4$. As results, the MB degradation is enhanced.

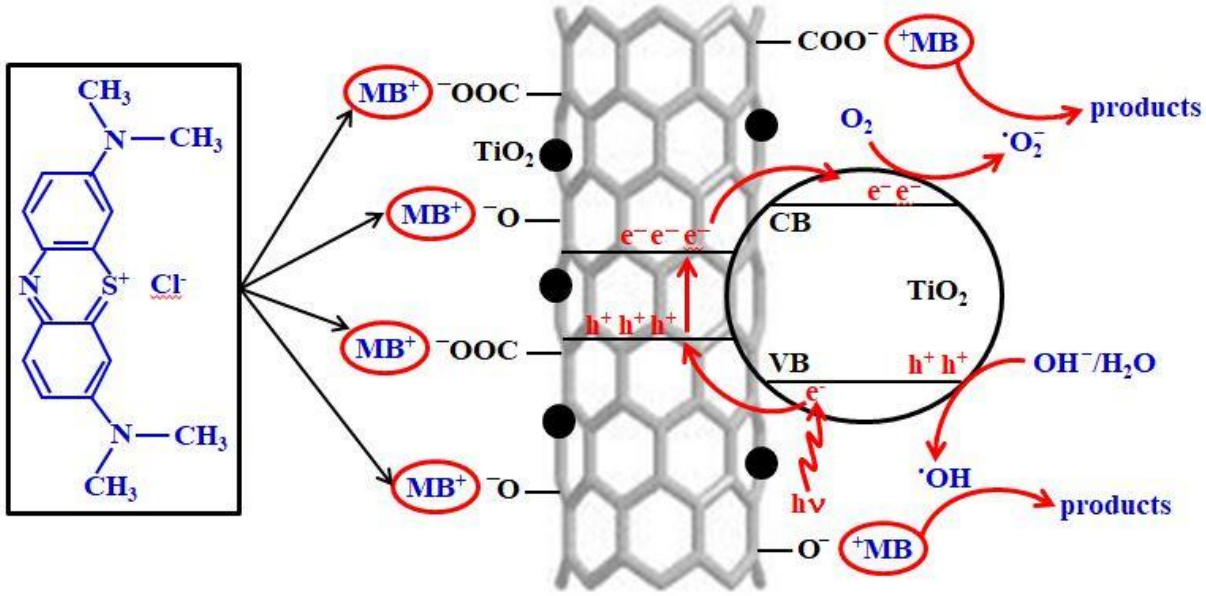

Scheme 2: The proposed mechanism of MB degradation over TiO_2/CNTs composite

4. CONCLUSION

TiO_2/CNTs composite was found to be an efficient photocatalyst for the degradation of methylene blue in aqueous solution. Anatase-TiO_2 is favourably formed at hydrolysis pH of 8 and highly dispersed on carbon nanotubes after 2 hours of ultrasonic treatment. More than 95 % of MB with initial MB concentration of 20 mg L^{-1} was removed at ambient temperature with the catalyst TiO_2/CNT at pH of 8 and catalyst dosage of 1.5 g L^{-1} after 90 min irradiation. The photocatalytic degradation mechanism of MB on the TiO_2/CNTs catalyst followed the Langmuir-Hinshelwood model. Kinetic study indicates that the intermediate between MB and catalyst is formed prior to the decomposition. Thermodynamic parameters confirmed the spontaneousness and endothermic nature of MB degradation.

REFERENCES

1. H. Dong, G. Zeng, L. Tang, C. Fan, C. Zhang, X. He. An overview on limitations of TiO_2-based particles for photocatalytic degradation of organic pollutants and the corresponding countermeasures, *Water Res.*, **2015**, *79*, 128-146.
2. L. Jiang, Y. Wang, C. Feng. Application of photocatalytic technology in environmental safety, *Procedia Eng.*, **2012**, *45*, 993-997.
3. H. L. Li, L. X. Cao, W. Liu, G. Su, B. H. Dong. Synthesis and investigation of TiO_2 nanotube arrays prepared by anodization and their photocatalytic activity, *Ceram. Int.*, **2012**, *38(7)*, 5791-5797.
4. Y. Li, Y. Wang, J. Kong, H. Jia, Z. Wang. Synthesis and characterization of carbon modified TiO_2 nanotube and photocatalytic activity on methylene blue under sunlight, *Appl. Surf. Sci.*, **2015**, *344*, 176-180.
5. J. Moma, J. Baloyi. Modified titanium dioxide for photocatalytic applications in Photocatalyst-Applications and Attributes, Intechopen, **2018**.
6. B. Szczepanik. Photocatalytic degradation of organic contaminants over clay-TiO_2 nanocomposites: A review, *Appl. Clay Sci.*, **2017**, *141*, 227-239.
7. J. Low, B. Cheng, J. Yu. Surface modification and enhanced photocatalytic CO_2 reduction performance of TiO_2: A review, *Appl. Surf. Sci.*, **2017**, *392*, 658-686.
8. J. Wen, X. Li, W. Li, Y. Fang, J. Xie, Y. Xu. Photocatalysis fundamentals and surface modification of TiO_2 nanomaterials, *Chinese J. Catal.*, **2015**, *36*(*12*), 2049-2070.
9. R. Daghrir, P. Drogui, D. Robert. Modified TiO_2 for

environmental photocatalytic applications: A review, *Ind. Eng. Chem. Res.*, **2013**, *52*(*10*), 3581-3599.

10. K. Woan, G. Pyrgiotakis, W. Sigmund. Photocatalytic carbonnanotube-TiO_2 composites, *Adv. Mater.*, **2009**, *21*, 2233-2239.
11. R. Leary, A. Westwood. Carbonaceous nanomaterials for the enhancement of TiO_2 photocatalysis, *Carbon*, **2011**, *49*, 741-772.
12. W. Wang, P. Serp, P. Kalck and J. L. Faria. Visible Light Photodegradation of Phenol on MWNT-TiO_2 Composite Catalysts Prepared by a Modified Sol-Gel Method, *J. Mol. Catal. A: Chem.*, **2005**, *235(1-2)*, 194-199.
13. W. Phang, M. Tadokoro, J. Watanabe and N. Kuramoto. Synthesis, characterization and microwave absorption property of doped polyaniline nanocomposites containing TiO_2 nanoparticles and carbon nanotubes, *Synth. Met.*, **2008**, *158*(*6*), 251-258.
14. A. Jitianu, T. Cacciaguerra, R. Benoit, S. Delpeux, F. Beguin, S. Bonnamy. Synthesis and characterization of carbon nanotubes-TiO_2 Nanocomposites, *Carbon*, **2004**, *42*, 1147-1151.
15. X-B. Yan, B. K. Tay, and Y. Yang. Dispersing and Functionalizing Multiwalled Carbon Nanotubes in TiO_2 Sol, *J. Phys. Chem. A*, **2006**, *110*, 25844-25849.
16. L. Tian, L. Ye, K. Deng, L. Zan. TiO_2/carbon nanotube hybrid nanostructures: Solvothermal synthesis and their visible light photocatalytic activity, *J. Solid State Chem.*, **2011**, *184*, 1465-1471.
17. V. R. Djokic, A. D. Marinkovic, M. Mitric, P. S. Uskokovic, R. D. Petrovic, V. R. Radmilovic, D. T. Janackovic. Preparation of TiO_2/carbon nanotubes photocatalysts: The influence of the method of oxidation of the carbonnanotubes on the photocatalytic activity of the nanocomposites, *Ceram. Int.*, **2012**, *38*, 6123-6129.
18. B. Kitiyanan, W. E. Alvarez, J. H. Harwell, D. E. Resasco. Controlled production of single-wall carbon nanotubes by catalytic decomposition of CO on bimetallic Co–Mo catalysts, *Chem. Phys. Lett.*, **2000**, *317*, 497-503.
19. C. L. Cheung, A. Kurtz, H. Park and C. M. Lieber. Diameter-Controlled Synthesis of Carbon Nanotubes, *J. Phys. Chem. B*, **2002**, *106*(*10*), 2429-2433.
20. U. C. Chung. Effect of H_2 on formation behavior of carbon nanotubes, *Bull. Korean Chem. Soc.*, **2004**, *25*(*10*), 1521-1524.
21. A. Firouzi, S. Sobri, F. M. Yasin, F. L. R. Ahmadun. Synthesis of carbon nanotubes by chemical vapor deposition and their application for CO_2 and CH_4 detection, *Int. Proc. Chem., Bio. Environ. Eng.*, **2011**, *2*, 169-172.
22. Y. S. Shin, J. Y. Hong, D. H. Ryu, M. H. Yum, J. H. Yang and C-Y. Park. The Role of H_2 in the Growth of Carbon Nanotubes on an AAO Template, *J. Korean Phys. Soc.*, **2007**, *50*(*4*), 1068-1072.
23. D. V. Q. Nguyen, Q. K. Dinh, N. T. Tran, X. T. Dang, and T. H. D. Bui. Carbon Nanotubes: Synthesis via Chemical Vapour Deposition without Hydrogen, Surface Modification, and Application, *J. Chem.*, **2019**, *2019*.
24. P. Srinivasu, S. P. Singh, A. Islam, and L. Han. Novel Approach for the Synthesis of Nanocrystalline Anatase Titania and Their Photovoltaic Application, *Adv. Optoelectron.*, **2011**, *2011*.
25. H. Ijadpanah-Saravy, M. Safari, A. Khodadadi-Darban & A. Rezaei. Synthesis of Titanium Dioxide Nanoparticles for Photocatalytic Degradation of Cyanide in Wastewater, *Anal. Lett.*, **2014**, *47*, 1772-1782.
26. Z. Jian & W. Hejing. The physical meanings of 5 basic parameters for an X-ray diffraction peak and their application, *Chin. J. Geochem.*, **2003**, *22(1)*, 38-44.
27. A. Escobedo-Morales, I. I. Ruiz-López, M.deL. Ruiz-Peralta, L. Tepech-Carrillo, M. Sánchez-Cantú, J. E. Moreno-Orea. Automated method for the determination of the band gap energy of pure and mixed powder samples using diffuse reflectance spectroscopy, *Heliyon*, **2019**, *5*(*4*), e01505.
28. M. Barberio, P. Barone, A. Imbrogno, S. A. Ruffolo, M. L. Russa, N. Arcuri and F. Xu. Study of Band Gap of Carbon Nanotube-Titanium Dioxide Heterostructures, *J. Chem. Chem. Eng.*, **2014**, *8*, 36-41.
29. M. M. Ayad, and A. B. El-Nasr. Adsorption of cationic dye (Methylene blue) from water using polyaniline nanotubes base, *J. Phys. Chem. C*, **2010**, *114*, 14377-14383.
30. D. V. Bavykin, E. V. Milsom, F. Marken, D. H. Kim, D. H. Marsh, D. J. Riley, F. C. Walsh, K. H. El-Abiary, A. A. Lapkin. A novel cation-binding TiO_2 nanotube substrate for elctro- and bioelectro-catalysis, *Electrochem. Commun.*, **2005**, *7*, 1050-1058.
31. D. V. Q. Nguyen, N. T. Tran, Q. K. Dinh, V. M. H. Ho, X. T. Dang, and K. Itatani. Oxidation of dibenzothiophene using the heterogeneous catalyst of tungsten-based carbon nanotubes, *Green Process. Synth.*, **2019**, *2019*.
32. C. Yang, W. Dong, G. Cui, Y. Zhao, X. Shi, X. Xia, B. Tang and W. Wang. Highly efficient photocatalytic degradation of methylene blue by P2ABSA-modified TiO_2 nanocomposite due to the photosensitization synergetic effect of TiO_2 and P2ABSA, *RSC Adv.*, **2017**, *7*(*38*), 23699-23708.
33. S. Bougarrani, K. Skadell, R. Arndt, M. Azzouzi, R. Gläser. Novel Ca_xMnO_y/TiO_2 composites for efficient photocatalytic degradation of methylene blue and the herbicide imazapyr in aqueous solution

under visible light irradiation, *J. Environ. Chem. Eng.*, **2018**, *6(2)*, 1934-1942.

34. F. Bairamis, I. Konstantinou, D. Petrakis, T. Vaimakis. Enhanced performance of electrospun nanofibrous TiO_2/g-C_3N_4 photocatalyst in photocatalytic degradation of methylene blue, *Catalysts*, **2019**, *9*(*11*), 880-893.
35. R. Kumar, J. Rashid, M. A. Barakat. Zero valent Ag deposited TiO_2 for the efficient photocatalysis of methylene blue under UV-C light irradiation, *Colloids Interface Sci. Commun.*, **2015**, *5*, 1-4.
36. W-C. Oh and M-L. Chen. Synthesis and Characterization of CNT/TiO_2 Composites Thermally Derived from MWCNT and Titanium(IV) *n*-Butoxide, *Bull. Korean Chem. Soc.*, **2008**, *29*(*1*), 159-166.
37. A. Houas, H. Lachheb, M. Ksibi, E. Elaloui, C. Guillard, J-M. Herrmann. Photocatalytic degradation pathway of methylene blue in water, *Appl. Catal. B: Environ.*, **2001**, *31*(*2*), 145-157.

Corresponding author: **Nguyen Duc Vu Quyen**
University of Sciences - Hue University
77, Nguyen Hue Str., Hue City, Thua Thien Hue 49000, Viet Nam
E-mail: ndvquyen@hueuni.edu.vn
Tel: +84- 979590971.